Effect of sintering temperature on the structure and properties of *in situ* synthesized B_4C-TiB_2 composites

Fuguan Peng*, Hong Shi, Jieqi Zhang

Jiangxi Polytechnic University, Jiujiang 332900, PR China

Received 29 October 2025; received in revised form 22 January 2026; accepted 27 February 2026

Abstract

Boron carbide (B_4C) ceramics, owing to their ultra-high hardness, low density and excellent neutron absorption capability, have significant potential in applications such as armour, nuclear industry and cutting tools. However, their inherently low fracture toughness at ambient temperature and difficulty in achieving full densification during sintering limit broader utilisation. In this study, TiB_2 reinforcement phases were fabricated in situ within B_4C via high-temperature and high-pressure sintering. The influence of sintering temperature on the phase composition, microstructure and mechanical properties of the B_4C-TiB_2 composites was systematically investigated to optimise the sintering process and performance. The results indicate that, with increasing sintering temperature, Ti progressively reacts with B_4C to form TiB_2, achieving complete Ti consumption at 1300 °C. At 1500 °C, the composites exhibited optimal performance: relative density of 99.6 %TD, Vickers hardness of 35.2 GPa, flexural strength of 694.6 MPa, and fracture toughness of 8.2 MPa·m$^{1/2}$. Further temperature increase to 1600 °C led to abnormal grain coarsening and consequent properties degradation. High-temperature and high-pressure sintering combined with in situ reaction enables the fabrication of highly dense, high-performance B_4C-TiB_2 composites, with temperature of 1500 °C identified as the optimal sintering temperature. This work provides not only a viable pathway for manufacturing, but also a theoretical basis for designing high-performance B_4C composites.

***Keywords**: B_4C-TiB_2 composite, high-temperature, high-pressure sintering, mechanical properties*

I. Introduction

Boron carbide (B_4C), owing to its ultra-high hardness, low density, excellent neutron absorption capacity and corrosion resistance, possesses unique application value in extreme environments such as armour protection, nuclear waste management and high-temperature cutting tools [1–4]. However, B_4C suffers from two critical drawbacks: i) low fracture toughness at ambient temperature, making it prone to brittle fracture under stress concentration; and ii) difficulty in achieving full densification during sintering [5,6]. Conventional sintering techniques, such as hot pressing and spark plasma sintering (SPS), require extremely high sintering temperatures combined with prolonged holding durations to obtain highly dense B_4C ceramics [7–13]. Such high-temperature, long-duration processing inevitably leads to the rapid grain coarsening, thereby degrading the mechanical performance of B_4C and significantly increasing manufacturing costs. Therefore, enhancement of the sintering behaviour of B_4C and reduction of the required sintering temperature are crucial to further expand its engineering applications.

High-temperature, high-pressure (HTHP) sintering technology, as an emerging material fabrication method, has attracted extensive attention from researchers. Owing to its advantages such as simple operation, reduction of sintering temperature, effective suppression of grain growth and promotion of rapid densification of the sintered body, the HTHP sintering has been widely applied in the fields of material synthesis and densification [14–16]. In addition, the introduction of high-performance secondary phases as reinforcement can further enhance the sintering behaviour and mechanical properties of B_4C ceramics. For example, Zhao *et al*. [12] prepared B_4C-TiB_2 composite ceramics via spark plasma sintering (SPS), achieving a fracture toughness of 5.28 MPa·m$^{1/2}$, Zhang *et al.* [7] fabricated B_4C-TiB_2-SiC composite ceramics using hot pressing, with fracture toughness ranging from 5.11 to 6.38 MPa·m$^{1/2}$, whereas Zhu *et al.* [17] produced B_4C-SiC-CeO_2 composite ceramics through pressureless sintering, obtaining a fracture toughness of 4.32 MPa·m$^{1/2}$. Among these

*Corresponding author: tel: +86 13705187680
e-mail: *pengfuguan@163.com*

reinforcements, TiB_2 exhibits excellent lattice matching with B_4C, low interfacial bonding energy and high hardness, making it an ideal reinforcement phase. B_4C-TiB_2 composites combine the ultra-high hardness of B_4C with the high toughness of TiB_2, representing a class of composite materials with significant application potential.

Therefore, in this work, dense B_4C-based composites were fabricated via high-temperature and high-pressure (HTHP) sintering, employing micron-sized Ti powder as the raw material to achieve *in situ* synthesis of TiB_2 within the B_4C matrix, characterised by fine grain size and uniform distribution. The influence of sintering temperature on the phase composition, microstructure and mechanical properties of B_4C-TiB_2 composites was systematically investigated.

II. Experimental

2.1. Sample preparation

In this work, 85 wt.% B_4C powder (particle size 2–3 μm, purity >99.9% Shanghai Aladdin Biochemical Technology Co., Ltd.) and 15 wt.% Ti powder (particle size 1–3 μm, purity >99.6% Shanghai Aladdin Biochemical Technology Co., Ltd.) were used as raw materials. The powders were weighed according to the designated proportions and placed into a stainless-steel milling jar together with cemented carbide balls and an appropriate amount of anhydrous ethanol. The ball-to-powder mass ratio was set to 5:1, the milling speed to 250 r/min and mixing was performed continuously for 2 h. After mixing, the slurry was dried and the mixed powder was transferred into a high-temperature vacuum tube furnace for vacuum heat treatment at 400 °C for 1 h. The heat-treated powder was then put into a molybdenum metal cup and assembled with pyrophyllite blocks according to the method described in the literature [18]. Finally, the samples were sintered in a six-anvil high-pressure apparatus under high-temperature and high-pressure conditions. The processing parameters were: pressure 5 GPa, temperature 800–1600 °C and holding time 8 min.

2.2. Sample characterisation

The relative density and porosity of the sintered samples were measured using the Archimedes water displacement method. Phase composition was characterised by X-ray diffraction (XRD) with a scanning rate of 5 °/min. Microstructural morphology was examined using field-emission scanning electron microscopy (SEM), and elemental analysis was performed via energy-dispersive spectroscopy (EDS). Vickers microhardness and fracture toughness were determined concurrently by the indentation method, applying a load of 3 kg and a dwell time of 15 s on polished surfaces, with five measurements taken per sample group. Fracture toughness (K_{IC}), of the B_4C ceramics after the indentation was calculated using the following equation [19]:

$$K_{IC} = 0.203 \cdot \left(\frac{c}{a}\right)^{-3/2} \sqrt{a} \cdot H_V \quad (1)$$

Here H_V is the hardness, a is the impression radius and c is the radial/median crack length. Flexural strength was tested by the three-point bending method, with a span length of 20 mm and a loading rate of 0.5 mm/min, also with five measurements per group. Sample dimensions were 25 × 3 × 2 mm.

III. Results and discussion

3.1. Phase analysis

Figure 1 shows the phase analysis of *in situ* fabricated B_4C-based composites at different temperatures. The synthesised composites are primarily composed of B_4C, TiB_2 and small amounts of B_2O_3, TiO_2 and free carbon. As observed, the reaction between Ti and B_4C begins to produce TiB_2 diffraction peaks at 1000 °C. With increasing sintering temperature, the diffraction peaks of Ti gradually decrease and completely disappear at 1300 °C, while the diffraction peaks of TiB_2 begin to intensify markedly from 1300 °C. A lower initiation temperature of the reaction (1000 °C) facilitates the formation of refined TiB_2 grains during subsequent sintering, thereby enhancing densification behaviour and mechanical properties. Conversely, an excessively high initiation temperature may induce coarsening of TiB_2 grains, compromising the strengthening effect. During the sintering, elevated temperatures accelerate atomic diffusion rates, thereby promoting chemical reactions. At lower sintering temperatures, Ti exists in the metallic elemental form within the composites, with relatively strong diffraction peaks; as the temperature increases to around 1300 °C, Ti reacts with B_4C to form TiB_2, a reinforcement phase with high hardness and high melting point. At this stage, the characteristic diffraction peaks of Ti gradually weaken until disappearing, whereas the newly formed TiB_2 peaks strengthen significantly. Additionally, small amounts of B_2O_3 and TiO_2 are by-products generated via oxidation of boron or titanium in the system, and the presence of free carbon originates from the decomposition of B_4C raw materials. Due to its low melting point, B_2O_3 may form a transient liquid phase during sintering, which can aid in particle rearrangement and densification. Free carbon may segregate to the grain boundaries, potentially hindering grain boundary diffusion and slightly inhibiting grain growth. However, if there is an excess of free carbon, it could also weaken grain boundary cohesion. Nevertheless, given the very low intensity of their

XRD peaks, we postulate that the content of these by-products is minimal, and their negative impact is negligible, exerting no significant effect on the mechanical properties of the sample. The acceleration of atomic diffusion at high temperatures is the key factor driving chemical reaction. High temperature supplies sufficient activation energy, enabling Ti atoms to diffuse rapidly into the B_4C lattice and form new compounds, thereby efficiently generating the TiB_2 reinforcement phase and improving the mechanical and physical properties of the composites.

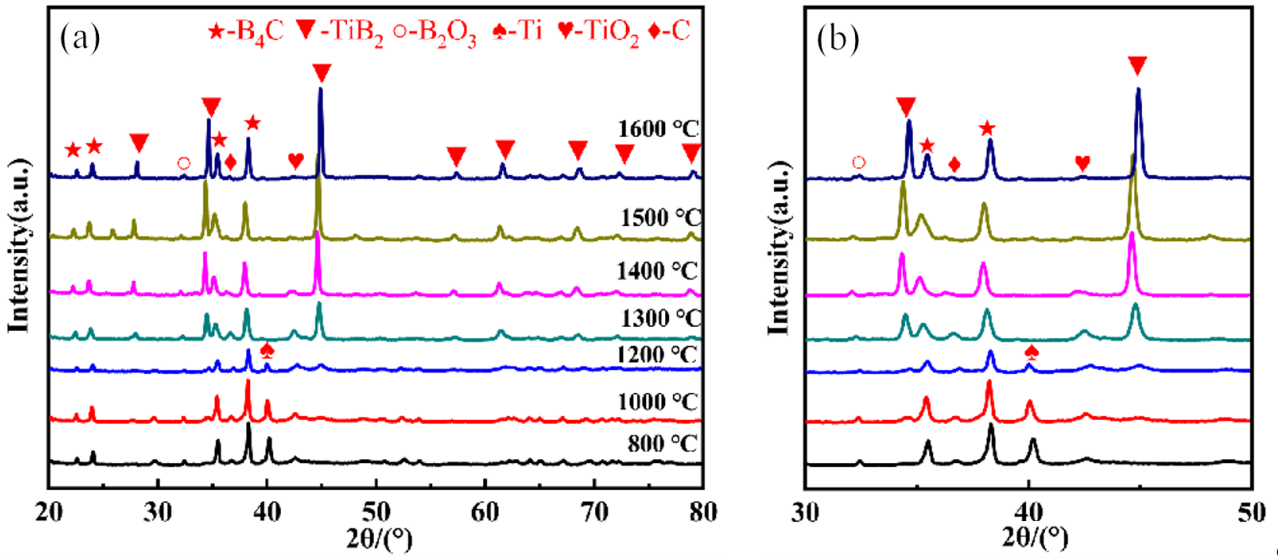

Figure 1. XRD patterns of samples sintered at different temperatures in the 2θ ranges of: a) 20–80° and b) 30–50°

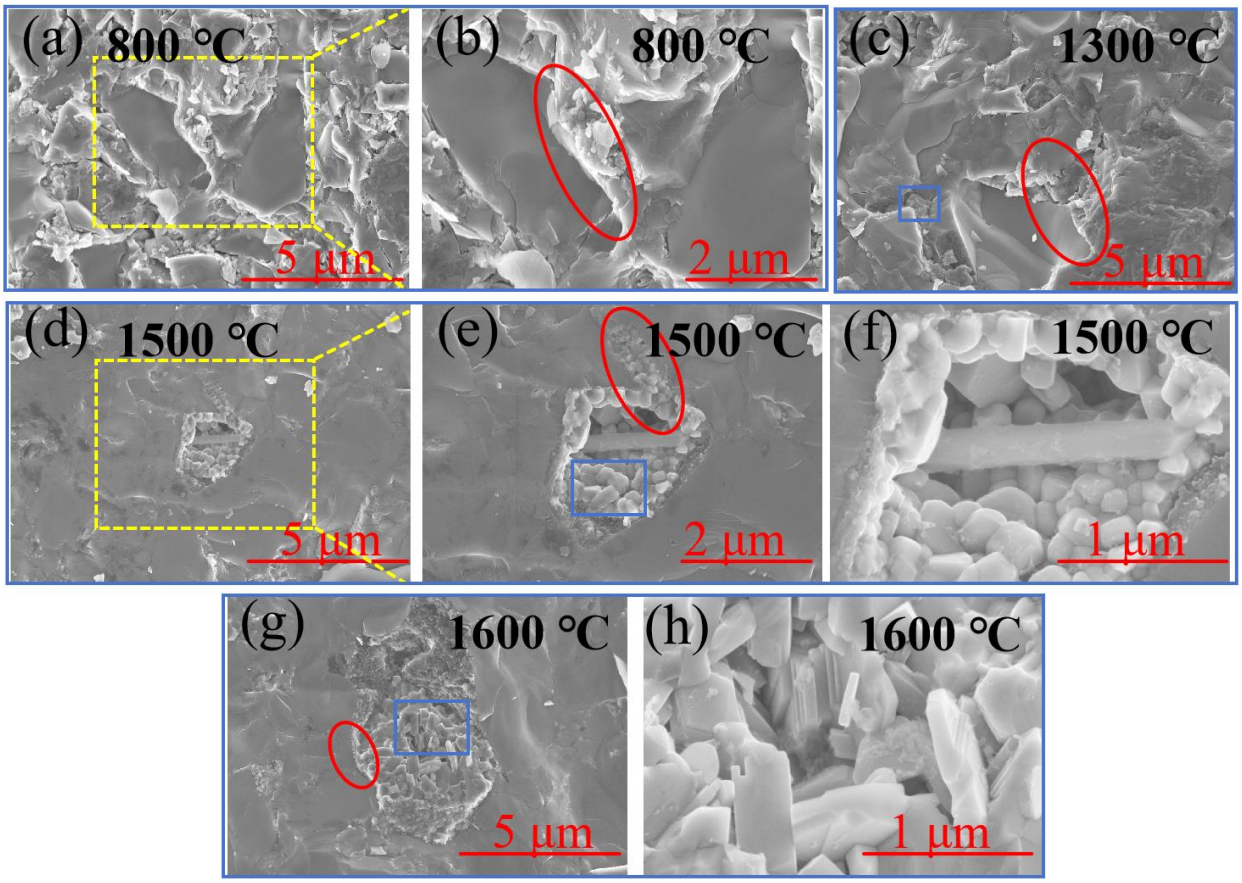

Figure 2. SEM micrographs of: (a,b) sample sintered at 800 °C exhibiting a loose structure and weak interfacial bonding, (c) sample sintered at 1300 °C showing reduced porosity and improved interfacial bonding, (d,e,f) sample sintered at 1500 °C with increased grain size and a dense structure and (g,h) sample sintered at 1600 °C exhibiting abnormal grain growth

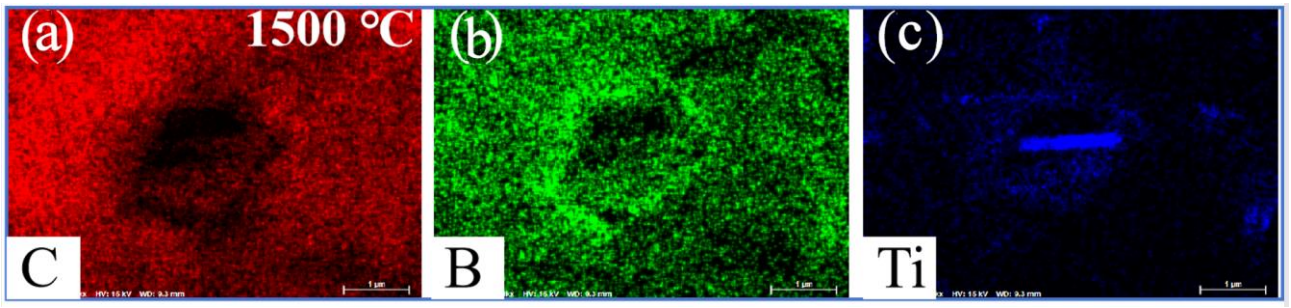

Figure 3. EDS elemental distribution analysis of the sample sintered at 1500 °C

3.2. Microstructure analysis

Figure 2 presents the cross-sectional SEM images of the B_4C-based composites prepared at different temperatures. As shown in Figs. 2a-h, with increasing temperature, the various phases within the specimens become progressively more compact. From Figs. 2a,b, it can be seen that the microstructure of the sample sintered at 800 °C is relatively loose, with numerous pores and non-uniformly distributed particles, i.e. interparticle bonding is weak. This is primarily attributed to insufficient sintering driving force at lower temperatures, resulting in slow diffusion between particles, inadequate to form strong bonds, leaving a large number of closed and open pores throughout the material, and leading to low overall densification. When the temperature is raised to 1300 °C (Fig. 2c), the densification is improved, pores are reduced and particles bonding becomes tighter. The increase in temperature provides a greater sintering driving force, promoting atomic diffusion and migration on particles' surfaces, allowing particles to gradually approach and form contact. Local grain growth is observed, but some pores and microcracks remain, as indicated by the red circles and blue rectangles. These pores result from the evaporation of volatile constituents or localised shrinkage heterogeneity during sintering, while the microcracks arise from stress concentration during grain growth. With a further temperature increase to 1500 °C (Figs. 2d,e,f), the microstructure becomes more densified, grain size increases and distribution becomes relatively uniform. Grain boundary bonding is tighter, with a significant reduction in porosity, as marked by the red circles and blue rectangles. Under these high-temperature conditions, mass transport processes are further accelerated, effectively eliminating residual pores where grains tend to arrange uniformly during growth. Upon raising the sintering temperature to 1600 °C (Figs. 2g,h), the microstructure becomes highly densified, grain size increases further and pores are almost completely eliminated, as indicated by the red circles and blue rectangles. Grain boundaries exhibit very tight bonding, forming a continuous and integrated structure. However, abnormal grain growth occurs at this stage, which may adversely affect mechanical properties. Excessive grain growth reduces grain boundary area, thereby weakening grain boundary strengthening, while large grains may contain more internal defects such as dislocations and vacancies. These defects can act as initiation sites for crack nucleation and propagation, reducing the strength, toughness and hardness of the material. Elemental distribution of the sample sintered at 1500 °C was determined by EDS analysis and shown in Fig. 3.

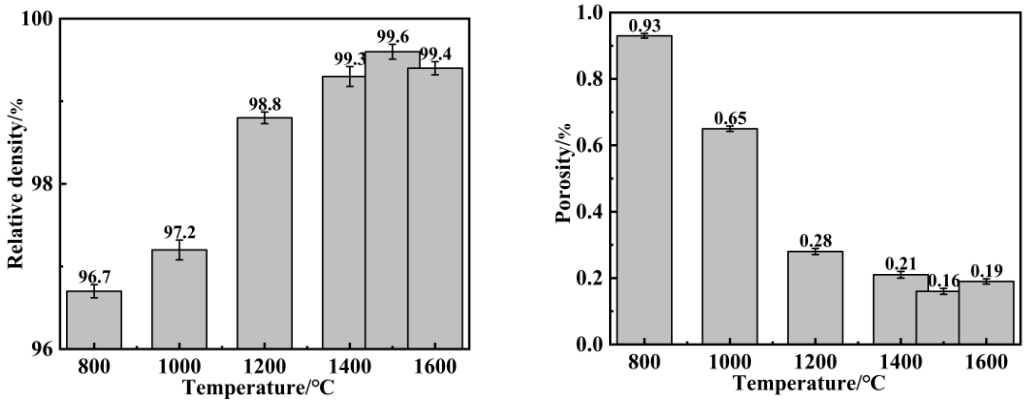

Figure 4. Relative density (a) and porosity (b) of samples sintered at different temperatures

3.3 Relative density and porosity

Figure 4 shows the relative density and porosity of the *in situ* fabricated B_4C-based composites at different temperatures. As indicated in Fig. 4, the relative density first increases and then decreases, while the porosity first decreases and then increases.

At 800 °C, the relative density of the fabricated ceramics is only 96.7 %TD, with a porosity of 0.93%. As the sintering temperature increases from 800 °C to 1500 °C, the degree of densification is significantly enhanced, with the relative density gradually rising and reaching a maximum value of 99.6 %TD at 1500 °C, accompanied by a minimum porosity of 0.16%. When the sintering temperature is further raised to 1600 °C, the relative density starts to decline and the porosity increases. This is attributed to the excessive grain growth or coarsening of the secondary phase particles at elevated temperatures, which accelerates grain boundary diffusion. In addition, partial liquid-phase volatilisation or chemical reactions generate new micropore defects within the material, thereby reducing densification and increasing porosity. Furthermore, too high sintering temperature leads to the abnormal grain growth of the B_4C and TiB_2 matrix phases, reducing grain boundary area, hindering the densification process and exacerbating pore formation and retention.

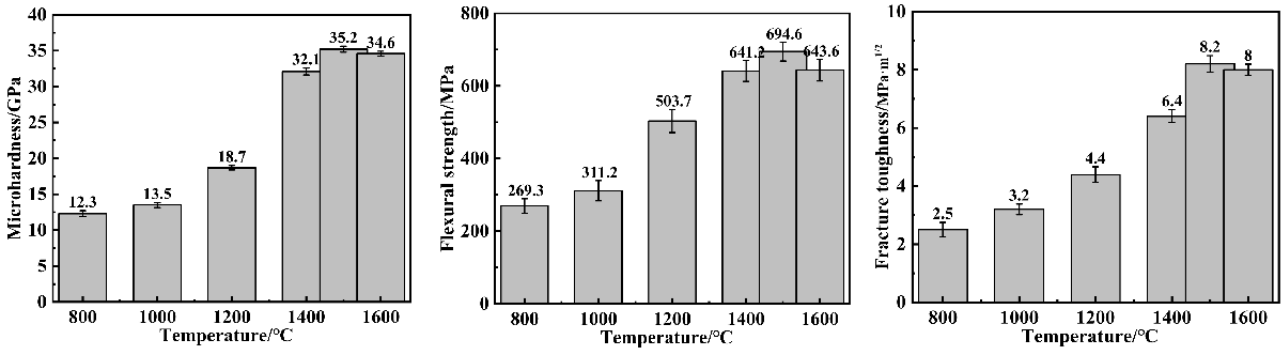

Figure 5. Mechanical properties of samples sintered at different temperatures: a) Vickers microhardness, b) flexural strength and c) fracture toughness

3.4. Mechanical properties

Figure 5 illustrates the effect of different sintering temperatures on the mechanical properties of the samples. As shown in Figs. 5a-c, the mechanical properties of the B_4C-based composites are significantly influenced by sintering temperature, exhibiting a trend of first increasing and then decreasing with temperature rising. When the sintering temperature increases from 800 to 1500 °C, the mechanical properties are markedly improved. The Vickers hardness rises from approximately 12.3 GPa to 35.2 GPa, the flexural strength increases from 289.7 MPa to 694.6 MPa and the fracture toughness improves from 2.5 MPa·$m^{1/2}$ to 8.2 MPa·$m^{1/2}$. This enhancement is attributed to the *in situ* formation of the TiB_2 reinforcement phase (with Ti diffraction peaks disappearing after 1300 °C) and the densification process during sintering, where the uniform distribution of TiB_2 and moderate grain size at 1500 °C synergistically yield optimal overall properties. At 1600 °C, excessive grain growth results in a decline in mechanical properties, with the Vickers hardness, fracture toughness and flexural strength measuring 34.6 GPa, 8.0 MPa·$m^{1/2}$ and 659.1 MPa, respectively. During sintering, increased temperatures promote reactions between Ti and B_4C to generate TiB_2, a high-hardness and high-strength reinforcement phase that effectively impedes dislocation motion, thereby enhancing hardness and flexural strength. Elevated temperatures also facilitate densification by reducing internal porosity, which not only improves relative density but also optimises crack propagation paths, thus increasing fracture toughness. At 1500 °C, TiB_2 forms a uniformly dispersed distribution with fine grain size that provides effective strengthening without inducing stress concentration, leading to the best combination of mechanical properties. However, further temperature increase to 1600 °C accelerates grain coarsening of both B_4C and TiB_2, diminishing grain boundary strengthening, reducing intergranular bonding strength and increasing the likelihood of crack propagation along grain boundaries, thus decreasing mechanical performance. Consequently, control of the sintering temperature to regulate grain size and the formation and distribution of reinforcement phases is a key strategy for optimising the mechanical properties of the B_4C-based composites, with 1500 °C identified as the optimal sintering temperature.

Figure 6a-f present SEM fractographs of the samples after three-point bending strength testing. Figure 6a shows that the fracture surface of the sample sintered at 800 °C contains numerous pores, and its microstructure exhibits a loose morphology. In contrast, the microstructures of the samples sintered at 1500 °C (Fig. 6b) and 1600 °C (Fig. 6c) display no obvious porosity defects, with fractures predominantly occurring along the B_4C matrix. This indicates that the B_4C phase plays a dominant role in the fracture process, and its intrinsic fracture characteristics significantly influence the overall fracture behaviour of the composite. Moreover, in the 1600 °C sintered sample, TiB_2 particles agglomeration and pronounced grain growth are more evident. Figures 6d,e show SEM images of the indentation-induced cracks in the 1500 °C sintered sample obtained after Vickers

hardness testing, while Fig. 6f provides a schematic of crack propagation. The images reveal typical toughening mechanisms during crack propagation, such as crack deflection and crack bridging. These microstructural features demonstrate that, during the crack advancement, these mechanisms can effectively dissipate the energy required for crack growth, thereby significantly enhancing the fracture toughness of the B_4C-based composites.

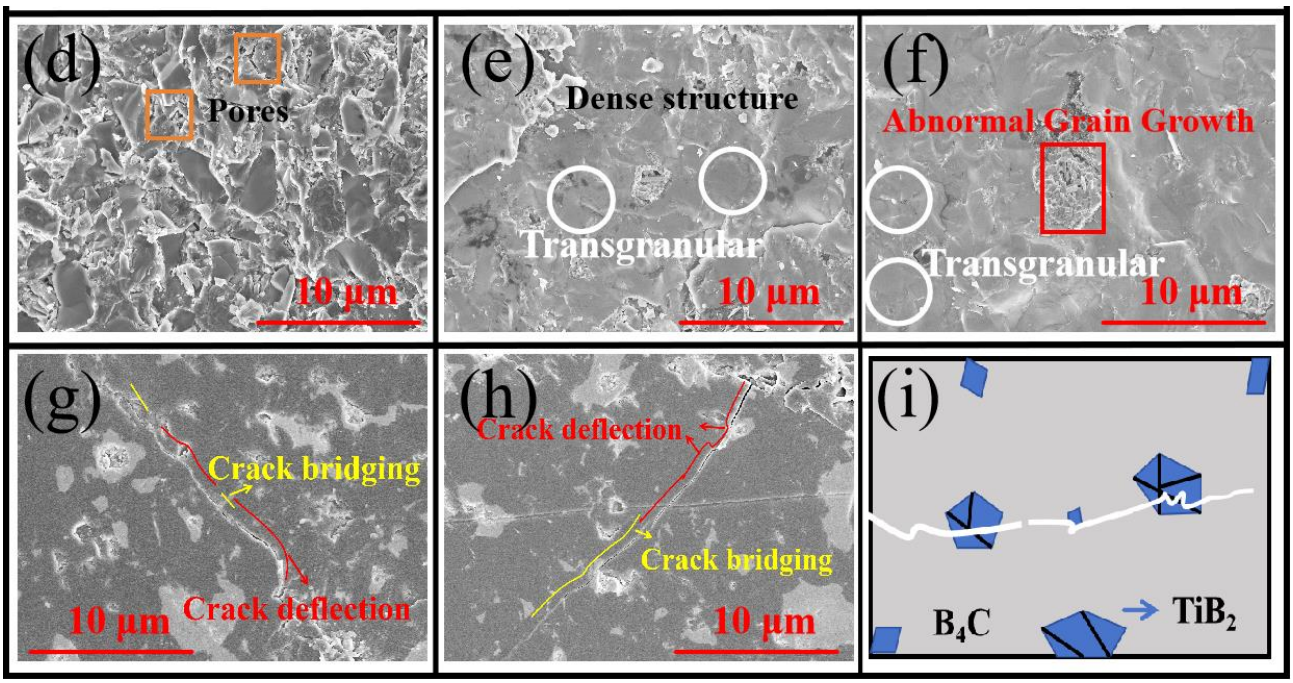

Figure 6. Fracture surface SEM images of samples sintered at: (a) 800 °C, (b) 1500 °C and (c) 1600 °C. SEM images of indentation-induced cracks in the sample sintered at 1500 °C (d,e) and scheme of crack deflection process

Table 1. Performance comparison of B_4C-based composites in recent years

References	Sintering temperature [°C]	Hardness [GPa]	Flexural strength [MPa]	Fracture toughness [MPa·m$^{1/2}$]
This work	1500 °	35.2	694.6	8.2
Zhao *et al.* [12]	2000	28.3	676	5.28
Ji *et al.* [19]	1700	33.5	506	5.5
Zhu *et al.* [8]	2150	27.5	336	5.11
Du *et al.* [20]	1750	27.7	474	5.08

Table 1 systematically compares the properties of B_4C ceramics prepared in recent years by methods such as SPS and pressureless sintering. The data indicate that conventional sintering requires exceeding an ultra-high temperature of 1700 °C to achieve full densification. This study innovatively employs an ultra-high pressure and high-temperature reactive sintering process (5 GPa/1500 °C), fabricating B_4C-TiB_2 composite ceramics via the *in situ* formation of nanosized TiB_2 from Ti. The resulting material exhibits excellent comprehensive properties. Firstly, the applied high pressure effectively suppresses grain growth, yielding a finer matrix grain size along with finer and more uniformly distributed TiB_2 particles. Secondly, the enhanced degree of densification minimises the detrimental effect of pores acting as crack initiation sites. Finally, the finely sized and well-dispersed TiB_2 particles, in combination with a clean and strongly bonded interface, effectively promote crack deflection and bridging mechanisms. These factors act synergistically to significantly enhance the mechanical performance of the fabricated samples.

IV. Conclusions

In this study, B_4C-TiB_2 composites were successfully fabricated via high-temperature and high-pressure sintering, and the effects of sintering temperature on phase evolution, microstructure and mechanical properties were systematically investigated. The conclusions are as follows:

(1) With increasing temperature, Ti undergoes an *in-situ* reaction with B_4C to form TiB_2. The reaction is essentially completed at 1300 °C, with Ti diffraction peaks disappearing and TiB_2 diffraction peaks significantly intensified.

(2) Elevated temperature promotes densification. At 1500 °C, the sample exhibits a dense structure with uniform grains, achieving a relative density of 99.6 %TD, while at 1600 °C, abnormal grain growth occurs and the densification level decreases.

(3) The sample sintered at 1500 °C demonstrates the optimal combination of mechanical properties: hardness of 35.2 GPa, flexural strength of 694.6 MPa and fracture toughness of 8.2 $MPa \cdot m^{1/2}$, attributed to the synergistic effect of uniformly distributed TiB_2 and a dense microstructure.

(4) Fractographic analysis and observation of indentation-induced cracks indicate that crack deflection and crack bridging are the key mechanisms for enhancing fracture toughness.

While this study focuses on the fundamental microstructure and room-temperature mechanical properties, future work will essential involve the evaluation of performance under extreme conditions, including thermal stability, high-temperature mechanical performance and corrosion resistance, to fully assess the material's application potential.

Acknowledgement: Supported by Science and Technology Research Project of Jiangxi Provincial Education Department, China (191283).

References

1. W. Guo, A. Wang, Q. He, T. Tian, C. Liu, L. Hu, Y. Shi, L. Liu, W. Wang, Z. Fu, "Microstructure and mechanical properties of B_4C-TiB_2 ceramic composites prepared via a two-step method", *J. Eur. Ceram. Soc*., **41** [14] (2021) 6952–6961.
2. A. Wang, L. Hu, W. Guo, X. Zhao, Y. Shi, Q. He, W. Wang, H. Wang, Z. Fu, "Synergistic effects of TiB_2 and graphene nanoplatelets on the mechanical and electrical properties of B_4C ceramic", *J. Eur. Ceram. Soc*., **42** [3] (2022) 869–876.
3. X. Zhang, Z. Zhang, W. Wang, X. Zhang, J. Mu, G. Wang, Z. Fu, "Preparation of B_4C composites toughened by TiB_2-SiC agglomerates", *J. Eur. Ceram. Soc*., **37** [2] (2017) 865–869.
4. Q. He, A. Wang, C. Liu, W. Wang, H. Wang, Z. Fu, "Microstructures and mechanical properties of B_4C-TiB_2-SiC composites fabricated by ball milling and hot pressing", *J. Eur. Ceram. Soc*., **38** [7] (2018) 2832–2840.
5. J. Zou, H.B. Ma, J.J. Liu, W.M. Wang, G.J. Zhang, Z.Y. Fu, "Nanoceramic composites with duplex microstructure break the strength-toughness tradeoff", *J. Mater. Sci. Technol*., **58** (2020) 1–9.
6. Y. Yuan, T.K. Ye, Y. Wu, Y. Xu, "Mechanical and ballistic properties of graphene platelets reinforced B_4C ceramics: Effect of TiB_2 addition", *Materi. Sci. Eng. A*, **817** (2021) 141294.
7. X.R Zhang, Z. Zhang, Y. Liu, A. Wang, S. Tian, W. Wang, J. Wang, "High-performance B_4C-TiB_2-SiC composites with tuneable properties fabricated by reactive hot pressing", *J. Eur. Ceram. Soc*., **39** [10] (2019) 2995–3002.
8. Y. Zhu, H. Cheng, Y. Wang, R. An, "Effects of carbon and silicon on microstructure and mechanical properties of pressureless sintered B_4C/TiB_2 composites", *J. Alloys Compd*., **772** (2019) 537–545.
9. S.M. So, W.H. Choi, K.H. Kim, J.S. Park, M.S. Kim, J. Park, Y.S. Lim, H.S. Kim, "Mechanical properties of B_4C-SiC composites fabricated by hot-press sintering", *Ceram. Int*., **46** [7] (2020) 9575–9581.
10. J. Sun, B. Niu, L. Ren, J. Zhang, L. Lei, F. Zhang, "Densification and mechanical properties of boron carbide prepared via spark plasma sintering with cubic boron nitride as an additive" *J. Eur. Ceram. Soc*., **40** [4] (2020) 1103–1110.
11. W.C. Guo, Q.L. He, A.Y. Wang, T. Tian, C. Liu, L. Hu, W. Wang, H. Wang, Z. Fu, "Effect of TiB_2 particles on microstructure and mechanical properties of B_4C-TiB_2 ceramics prepared by hot pressing", *Ceram. Int*., **49** [3] (2023) 4403–4411.
12. J. Zhao, D. Wang, X. Jin, X. Ding, J. Zhu, S. Ran, "Highly electro-conductive B_4C-TiB_2 composites with three-dimensional interconnected intergranular TiB_2 network", *J. Adv. Ceram*., **12** [1] (2023) 182–195.
13. J. Zhao, X.S. Zhang, Z.N. Ma, D. Wang, X. Jin, S. Ran, "Tuning mechanical and electrical performances of B_4C-TiB_2 ceramics in a two-step spark plasma sintering process", *J. Adv. Ceram*., **13** [4] (2024) 518–528.
14. J. Wang, D.L. Chu, H.G. Ma, S. Fang, Q. Chen, B. Liu, G. Ji, Z. Zhang, X. Jia, "Effect of sintering temperature on phase transformation behavior and hardness of high-pressure high-temperature sintered 10 mol% Mg-PSZ", *Ceram. Int.*, **47** [1] (2021) 15180–15185.
15. Y.P. Wang, Z.L. Kou, J.W. Zhang, S. Chen, L. Zhang, B. Peng, M. Zhao, M. Jiang, X. Yin, D. He, "A new pressurization-insulation and pre-sealing system to improve pressure in cubic press from 6 GPa to 12 GPa", *Rev. Sci. Instrum*., **91** [3] (2020) 035119.
16. M. Hu, N. Bi, M. Liu, S. Li, T. Su, G. Gao, Q. Hu, "Microstructure and performance of solidified TiB_2-TiC composites prepared by high pressure and high temperature", *J. Alloys Compd*., **786** (2019) 906–911.
17. Y. Zhu, F. Wang, Y. Wang, H. Cheng, D. Luo, Y. Zhao, "Mechanical properties and microstructure evolution of pressureless-sintered B_4C-SiC ceramic composite with CeO_2 additive", *Ceram. Int*., **45** [12] (2019) 15108–15115.
18. J. Zhang, F. Peng, H. Shi, P. Mo, "High pressure and low temperature in situ preparation of B_4C-TiB_2 composite ceramics with strengthening-toughening mechanisms", *J. Mater. Eng. Perform*., (2025) https://doi.org/10.1007/s11665-025-12419-4.
19. W. Ji, R.I. Tood, W. Wang, H. Wang, J. Zhang, Z. Fu, "Transient liquid phase spark plasma sintering of B_4C-based ceramics using Ti-Al intermetallics as sintering aid", *J. Eur. Ceram. Soc*., **36** [10] (2016) 2419–2426.
20. Z. Du, M. Yi, S. Chen, J. Zhang, G. Xiao, Z. Chen, H. Chen, C. Xu, "Toughening mechanism of B_4C/TiB_2 ceramic materials by in situ reaction via spark plasma sintering", *Int. J. Appl. Ceram. Technol*., **21** [5] (2024) 3462–3475.